Metallomics

Accepted Manuscript

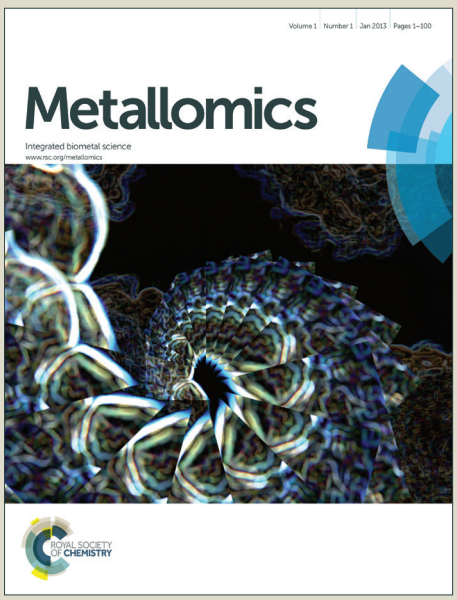

ROYAL SOCIETY OF CHEMISTRY

www.rsc.org/metallomics

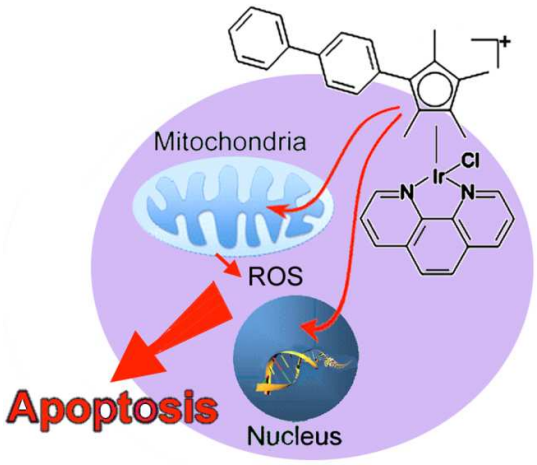

An iridium(III) complex $[(\eta^5\text{-}C_5Me_4C_6H_4C_6H_5)Ir(phen)Cl]PF_6$ (phen=phenanthroline) exhibits dual effects in killing cancer cells causing nuclear DNA damage and mitochondrial dysfunction simultaneously.

Metallomics

RSCPublishing

ARTICLE

A dual-targeting, apoptosis-inducing organometallic half-sandwich iridium anticancer complex†

Cite this: DOI: 10.1039/x0xx00000x

Received 00th January 2014,
Accepted 00th January 2014

DOI: 10.1039/x0xx00000x

www.rsc.org/

Vojtech Novohradsky,‡[ab] Lenka Zerzankova,‡[a] Jana Stepankova,[a] Anna Kisova,[a] Hana Kostrhunova,[a] Zhe Liu,[cd] Peter J. Sadler,[c] Jana Kasparkova,[b] and Viktor Brabec *[,a]

The cellular mechanism of action of iridium(III) half-sandwich complex [(η^5-$C_5Me_4C_6H_4C_6H_5$)Ir(phen)Cl]PF_6 (phen = phenanthroline) (**1**) is reported. Complex **1** was used to treat several cell lines, including cisplatin-sensitive, cisplatin-resistant (with intrinsic and acquired resistance) carcinoma cells with wild type p53 status as well as the cells with no intact p53 gene, and nontumorigenic cells. Complex **1** preferentially kills cancer cells over nontumorigenic cells and exhibits no cross-resistance with cisplatin. It appears to retain significant activity in human tumor cell lines that are refractory or poorly responsive to cisplatin, and in contrast to cisplatin it displays a high activity in human tumor cell lines that are characterized by both wild type and mutant p53 gene. The mechanism of cell killing was established through detailed cell-based assays. Complex **1** exhibits dual effects in killing cancer cells causing nuclear DNA damage and mitochondrial dysfunction involving ROS production simultaneously. Flow cytometric studies and impedance-based monitoring of cellular responses to **1** demonstrated that **1** acts more quickly than cisplatin to induce cell death and that **1** is more effective apoptosis inducer than cisplatin in particular in early stages of treatment, when the apoptotic effects predominate over necrosis. Overall, our findings confirm that **1** and its iridium derivatives represent promising candidates for further pre-clinical studies and new additions to the growing family of nonplatinum metal-based anticancer complexes.

Introduction

A large number of organometallic transition metal-based complexes have been designed and researched as anticancer agents.[1-4] Impetus to the design of such metallodrugs is provided by a need to produce compounds with higher potency, a wider spectrum of activity, higher cancer cell selectivity, lower resistance, and reduced side effects in comparison with conventional antitumor metal-based (platinum) drugs already used in the clinic. In this respect, the most widely researched anticancer metallodrugs are those derived from platinum and ruthenium complexes. Iridium complexes remain relatively unexplored (see[5-12] and references therein).

Quite recently, novel half-sandwich organometallic Ir^{III} cyclopentadienyl complexes as potent cytostatic and cytotoxic anticancer agents were introduced.[7] These pseudo-octahedral complexes have carbon-bound cyclopentadienyl ligands that occupy three coordination sites, an N,N- or C,N- chelating ligand that occupies the fourth and fifth sites, and a monodentate Cl ligand at the sixth site (see complex **1** in Fig. 1 as example). It has been shown[13] that these complexes exhibit higher potency than conventional cisplatin. Moreover, it was predicted with the aid of the National Cancer Institute COMPARE algorithm (which can provide insight into mechanism of action) that the mechanism underlying biological effects of these Ir^{III} complexes does not correlate to that of cisplatin. On the other hand, the COMPARE analysis predicted that **1** may belong to the class of DNA interacting compounds and protein synthesis inhibitors.[13]

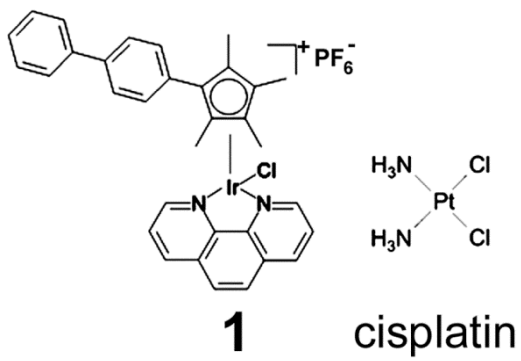

Fig. 1. Schematic representation of the metal complexes used in this work.

The results of previous initial studies aimed at probing this prediction[13] were consistent with the thesis that DNA interactions of **1** may be one of the factors involved in its mechanism of activity. More specifically, our previous work[7] has shown that the extent of binding of Ir from **1** to DNA in cells treated with this agent is ~6% of the total iridium taken up by the cells. This extent of metal binding to DNA is markedly higher than that reported for cisplatin (~1-2%) for which it is generally believed that DNA is the major pharmacological target.[14-16] In addition, it has been also shown that **1** in a cell-free medium can interact with DNA, binding both directly via Ir coordination to DNA bases and via intercalation of extended cyclopentadienyl ligands and that the molecules of this complex **1** bound to DNA can efficiently inhibit DNA synthesis by DNA polymerases.[17] Nevertheless, these results do not exclude an eventuality that the antineoplastic activity of **1** could also result from its interactions with other molecular targets. This suggestion is consistent with the COMPARE analysis[13] which predicted that **1**, in contrast to cisplatin, may also belong to the class of anticancer agents whose mechanism of action can be associated not only with DNA interaction, but also with protein synthesis disruption and redox mediation, all closely related to mitochondrial effects.

The aim of the present study was to further characterize the mechanism of biological activity of **1**, a representative of novel anticancer half-sandwich organometallic Ir^{III} cyclopentadienyl complexes, *in cellulo* to gain insight into its mechanism of action and polypharmacology. We have investigated cellular changes induced by **1** to determine experimentally possible response biomarkers and factors predictive of the activity of **1**.

Experimental

Chemicals

Ir^{III} half-sandwich complex $[(\eta^5\text{-}C_5Me_4C_6H_4C_6H_5)Ir(phen)Cl]PF_6$ (phen = phenanthroline) (**1**) was prepared by the methods described in detail previously.[7] Cisplatin and dimethyl sulfoxide (DMSO) were obtained from Sigma-Aldrich s.r.o., Prague, Czech Republic. The stock solutions of **1** and cisplatin were always freshly prepared in DMSO before use. The final concentration of DMSO in cell culture medium did not exceed 0.25% (v/v). Agarose, Nodidet NP-40, RNase A and proteinase K were purchased from Merck KgaA (Darmstadt, Germany), sodium dodecyl sulfate (SDS) from Serva (Heidelberg, Germany).

Cell lines

The human ovarian carcinoma cisplatin sensitive A2780 cells, cisplatin resistant A2780/cisR (cisplatin resistant variant ofA2780 cells), the human breast cancer MCF-7 cells and human leukemia HL-60cells were kindly supplied by Professor B. Keppler, University of Vienna (Austria). The Chinese hamster ovary CHO-K1 cells (wild type, non-carcinoma cells) were kindly supplied by Dr. M. Pirsel, Cancer Research Institute, Slovak Academy of Sciences, Bratislava (Slovakia). Human skin fibroblasts (primary cell culture) (HSF) was a kind gift from Professor T. Adam, Laboratory of Inherited Metabolic Disorders, Department of Clinical Chemistry, Palacky University and Hospital, Olomouc, Czech Republic. The A2780, A2780/cisR and HL-60 cells were grown in RPMI 1640 medium (PAA; Pasching, Austria) supplemented with gentamycin (50 $\mu g \cdot mL^{-1}$, Serva) and 10% heat inactivated fetal bovine serum (PAA; Pasching, Austria). The acquired resistance of A2780/cisR cells was maintained by supplementing the medium with 1 μM cisplatin every second passage. TheMCF7, CHO-K1 cells and human skin fibroblasts were grown in Dulbecco's modified Eagle's medium(DMEM) medium (high glucose, 4.5 $g \cdot L^{-1}$, (PAA; Pasching, Austria) supplemented with gentamycin (50 $\mu g \cdot mL^{-1}$, Serva) and 10%

heat inactivated fetal bovine serum (PAA; Pasching, Austria). V79 cells were grown in DMEM supplemented with gentamycin and 10% heat-inactivated fetal bovine serum (Carlsbad, CA).The cells were cultured in a humidified incubator at 37 °C in a 5% CO_2 atmosphere and subcultured 2-3 times a week with an appropriate plating density.

Cytotoxicity

Cell death was evaluated by using either an assay based on Sulforhodamine B (SRB) uptake, the tetrazolium compound MTT [3-(4,5-dimethyl-2-thiazolyl)-2,5-diphenyl-2H-tetrazolium bromide] metabolization or neutral red (NR, 2-amino-3-methyl-7-dimethyl-aminophenazomium chloride) uptake as described in the Supporting material. The adherent cells, A2780, A2780/cisR, CHO-K1, MCF-7 and skin fibroblasts were plated out 16 h prior to testing in 96-well tissue culture plates at a density of 10^4 A2780 or A2780/cisR cells/well or $6{\cdot}10^3$ CHO-K1 or MCF-7 cells/well in 100 µL of medium. The cells were treated with the compounds at the final concentrations in the range of 0 to 128 µM in a final volume of 200 µL/well. After the treatment period, viability of the cells was tested. Alternatively, for the suspension cell line HL-60, cells were seeded out at 10^3 cells/well in 50 µL medium immediately prior to testing. The cells were treated with the compounds at a final concentration in the range of 0 to 128 µM in a final volume of 100 µL/well. Cytotoxic effects were expressed as IC_{50} (compound concentrations that produce 50% of cell growth inhibition); IC_{50} values were calculated from curves constructed by plotting cell survival (%) versus drug concentration (µM). All experiments were made in triplicate.

Interaction of complex 1 and cisplatin with cells monitored by real-time cell electronic sensing

Background of the E-plates was determined in 100 µL of medium (RPMI), and subsequently, 50 µL of the A2780 cell suspension was added (10^4 cells/well). E-plates were immediately placed into the Real-time Cell Analyzer (RTCA) station (xCELLigence RTCASP Instrument, ROCHE). Cells were grown for 24 h (in a humidified incubator at 37 °C in a 5% CO_2). Subsequently, the cells were treated with 50 µL of media alone (control) or with 50 µL of medium containing varying inhibitory concentrations of **1** or cisplatin, and impedance was monitored for the first 6 h every 15 min and for the rest of the test period every 30min. The electronic readout, cell-sensor impedance, is displayed as an arbitrary unit called cell index (CI). CI at each time point is defined as (Rt−Rb)/15 where Rt is defined as the cell-electrode impedance of the well with the cells at different time points, and Rb is defined as the background impedance of the well with the medium alone. Normalized CI was calculated by dividing the cell index at particular time points by the CI at the time of interest. Each treatment was performed in triplicate.

DNA binding in cells

A2780 cells grown to near confluence were exposed to 5 µM **1** or cisplatin for 24 h. After incubation period cells were trypsinized and washed twice in ice-cold PBS. Cells were then lysed in DNAzol (DNAzol® genomic DNA isolation reagent, MRC) supplemented with RNAse A (100 $\mu g{\cdot}mL^{-1}$). The genomic DNA was precipitated from the lysate with ethanol, dried and resuspended in water. The DNA content in each sample was determined by UV spectrophotometry. To avoid an interference by the high DNA concentration on detection of iridium or platinum in the samples by inductively coupled plasma mass spectroscopy (ICP-MS), the DNA samples were digested in the presence of hydrochloric acid (11 M) using a high pressure microwave mineralization system (MARS5, CEM). Experiments were performed in triplicate and the values are the means ± SD.

FIT Cannexin V/dead cell apoptosis

Flow cytometry with a FITC Annexin V/Dead Cell Apoptosis Kit (with FIT Cannexin V and PI for Flow Cytometry, Invitrogen) was used to determine whether the treatment with **1** specifically induces apoptosis. A2780 or HL-60 cells were pretreated with or without **1** or, for comparative purposes, with cisplatin. At each time point, HL-60 cells were collected and washed twice in PBS (4 ºC). Cells were resuspended in Annexin-binding buffer ($1{\cdot}10^5$ cells/100 µL per assay) and subsequently stained by annexin V and propidium iodide as per manufacturer's protocol. Cells were analyzed immediately after staining by flow cytometry (BD FACS Aria II Sorter) and data were analyzed using (version 7.6.5). Dot plots representative of three independent experiments with similar results are shown.

DNA laddering assay

The convenient and successful method to detect DNA laddering in cells undergoing apoptosis developed by Gong et al.[18] was employed. Untreated or drug-treated cells were collected by centrifugation and resuspended in Hanks' buffered salt solution (HBSS). The cells were fixed in 70% ethanol by transferring 1 mL of cell suspension (approx. $3{\cdot}10^6$ cells in HBSS) into tubes containing 10 mL of 70% ethanol, on ice. The cells were stored at -20 °C for at least 24 h. The cells were then centrifuged at 800 g for 5 min and the ethanol was thoroughly removed. The cell pellets (approx. $3{\cdot}10^6$ cells) were resuspended in 40 µL of phosphate-citrate buffer [Na_2HPO_4 (0.192 M), citric acid (4 mM), pH 7.8], at room temperature, for at least 30 min. After centrifugation at 1000 g for 5 min, the supernatant was transferred to new tubes and concentrated by vacuum in a SpeedVac concentrator. A 3-µL aliquot of 0.25% Nonidet NP-40 in distilled water was then added, followed by 1 µL of a solution of RNase A (3 $mg{\cdot}mL^{-1}$ in water). After 30 min incubation at 37 °C, 1 µL of a solution of proteinase K (3 $mg{\cdot}mL^{-1}$) was added and the extract was incubated for additional 30 min at 37 °C. After the incubation loading buffer was added and the entire content of the tube was transferred to the gel. Horizontal 1.5% agarose gel electrophoresis was performed at 4 $V{\cdot}cm^{-1}$ for 4 h. The DNA in the gel was visualized under UV light after staining with 5 $\mu g{\cdot}mL^{-1}$ of ethidium bromide.

Cell cycle analysis

At each time point, A2780/HL-60 cells were collected (floating + attached), washed twice in PBS (4 ºC), fixed in 70% ethanol, and stored at 4 ºC. Cell pellets were subsequently rinsed with 0.5 mL PBS and 0.5 mL phosphate-citrate buffer [Na_2HPO_4 (0.2 M), citric acid (0.1 M), pH 7.8]. After 5 min incubation the cells were sedimented and stained with Vindel's solution [Tris-Cl (10 mM, pH 8.0), NaCl (10 mM), Triton X100 (0.1%), RNAse A (10 $\mu g \cdot mL^{-1}$, QIAGEN), propidium iodide (50 $\mu g \cdot mL^{-1}$)] for 1 h at 37 ºC in the dark. DNA content was measured using flow cytometry (BD FACS Aria II Sorter). The percentages of cells in the individual cell cycle phases were analyzed using ModFit 2.0 software (Verity Software House).

Cell death detection

Characteristics of the cell death were measured after treatment with **1** or cisplatin in A2780 or HL-60 cells. To identify whether the cell death is related to apoptotic or necrotic processes the level of cytoplasmic histone-associated DNA fragments (mononucleosomes and oligonucleosomes) was quantified by specific cell death detection ELISA plus kit (Roche Molecular Biochemicals, Mannheim, Germany) according to manufacturer's protocol. Briefly, the cells (10^4) were treated with equimolar (3 µM) or equitoxic (IC_{50}) concentrations of **1** or cisplatin for 24 h. After centrifugation (200 g), 20 µL of the supernatant was used in the ELISA for detection necrosis. Cells were resuspended in 200 µL of the lysis buffer contained in the kit and incubated for 30 min at room temperature. After pelleting the nuclei (200 g, 10 min), 20 µL of the supernatant (cytoplasmic fraction) was used in the ELISA for detection of apoptosis. Following incubation with peroxidase substrate for 15 min the absorbance was determined at 405 nm (reference 490 nm) with the fluorescence reader Infinite 200 (TECAN, Schoeller, Mannendorf, Germany). Signals from wells containing the substrate only were subtracted as background.

Multi-parameter-apoptosis assay

For phenotypic characterization of different cell death parameters at a single-cell level, multiparametric apoptosis assay kit (Cayman Chemical, Michigan, USA) was used according to the manufacturer's protocol. Briefly, A2780 cells (10^6 cells) were seeded on the 50 mm glass bottom culture dishes (P50G-0-30-F; Mattek, Ashland, USA) and incubated overnight. The cells were then treated with equitoxic concentrations (IC_{90}) of **1** (2.6 µM) or cisplatin (20 µM) for 48 h. After the treatment, the cells were stained with TMRE/Hoechst for 15 min (TMRE is tetramethylrhodamine, ethyl ester), centrifuged at 400g for 5 min. Samples were visualized by confocal fluorescence microscopy Leica TSC SP-5 X, sequentially scanned with the objective HCX PL APO lambda blue 63.0x1.20 water UV, corrected with an appropriate beam path (resolution 1024x1024, frequency 100 Hz). Excitation/emission wavelengths: Hoechst (355 /465 nm), TMRE (560 /595 nm).

Intracellular reactive oxygen species (ROS) determination

Intracellular ROS were quantified to determine the oxidative stress in A2780 cells after the treatment with **1** or cisplatin. The method developed by Robinson et al.[19-20] was used. A2780 cells ($2 \cdot 10^4$) were seeded on a 96-well black plates for 24 h. Then the cells were treated with various concentrations (0, 1, 5, 10, 20 µM) of complex **1** of cisplatin. Control, untreated cells contained maximal concentration of DMSO used in the treatment ($\leq$ 0.2%). The treated cells were loaded with 10 µM of DCFH-DA and incubated for 30 min. at 37 °C. The plates were washed with PBS and scanned on fluorescence reader Infinite 200 (TECAN) (excitation/emission wavelengths: 504nm/529nm). Experiments were repeated in triplicate.

Other physical methods

Absorption spectra were recorded using a Beckmann DU-7400 spectrophotometer. The analysis with the aid of ICP-MS was performed using an Agilent 7500 instrument (Agilent, Japan). Statistical evaluation of the untreated control cells and drug treated cells was carried out using Student's t-test. If not stated otherwise, all experiments were performed at least in triplicate.

Results

Antiproliferative effects of complex 1 in a panel of cancer and nontumorigenic cell lines

The cytotoxic activity of **1** and cisplatin was determined against a panel of cisplatin-sensitive and -resistant human cancer cell lines and the nontumorigenic, normal human fibroblast cells and Chinese hamster ovary cells (Table 1). The cell lines were incubated for 72 h with **1** or cisplatin. Several colorimetric assays can be used for *in vitro* chemosensitivity testing of tumor cell lines, although use of these assays has various advantages and limitations. It is so because the principles of these assays are differently dependent on metabolic and other factors and/or some compounds can directly interfere with reactions responsible for conversion of the colorless dye to the colored product without having any effects on cell viability which may, in turn, substantially affect the quantitation of cell viability.

The anti-proliferative properties of **1** and cisplatin were first evaluated by the sulforhodamine B (SRB) assay. Its principle is based on the ability of the protein dye sulforhodamine B to bind electrostatically to protein basic amino acid residues, which makes it possible to quantify cellular protein content of cultured cells.[21] The corresponding IC_{50} values are reported in Table 1.

We also compared the effectiveness of the SRB test to that of another methods using the tetrazolium dye MTT or the neutral red. The MTT assay requires cellular metabolic activity (measures mitochondria dehydrogenase activity as a marker of cell viability) to convert the colorless tetrazolium to the purple-colored formazan dye. Conversely, the neutral red

Metallomics

RSCPublishing

ARTICLE

Table 1. IC_{50} Mean Values (μM) obtained by SRB assay for **1** and cisplatin[a]

	A2780	A2780cisR[b]	HL-60	MCF-7	CHO-K1[b]	HSF[c]
1	0.22±0.03	0.42±0.03 (1.9)	0.28±0.05	0.84±0.08	12.0±0.3 (55)	5.48±0.37 (25)
cisplatin	0.81±0.19	3.80±0.20 (4.7)	1.58±0.48	9.26±1.21	6.45±0.49 (8)	14.2±1.6 (18)

[a]The experiments were performed in triplicate. The drug-treatment period was 72 h. The results are expressed as mean values ± SD for three independent samples.

[b]Resistance factor, defined as IC_{50} (resistant, A2780cisR)/IC_{50} (sensitive, A2780) is given in parentheses.

[c]Therapeutic Index calculated as a ratio of the $IC_{50}$of normal, noncancerous cells (CHO-K1 or HSF), to the IC_{50} obtained for cancer cells (A2780) is given in parentheses.

uptake assay is based on the ability of viable cells to incorporate and bind the dye in lysosomes by an active metabolic process. The results demonstrating the anti-proliferative properties of **1** and cisplatin determined by the MTT and neutral red assays are summarized in Tables S1 and S2, respectively. These studies undertaken by the different colorimetric assays show that results correlated well, although the IC_{50} values of compounds tested using the MTT method were slightly higher.

Impedance-based monitoring in real time of the effects on cell growth

Impedance-based time-dependent cell response profiling (TCRP) has been used to measure and characterize cellular responses to **1** in comparison with cisplatin. Interestingly, the TCRP of **1** shows significant differences from that of cisplatin, as shown in Fig. 2. The effect of cisplatin is characterized by an initial negligible increase in cell index in comparison with the control followed by a concentration dependent decrease in the cell index below control levels reflecting cytotoxic response. In contrast, treatment with **1** results in an immediate and more pronounced decrease in the cell index. Most strikingly, while **1** at the highest concentration (IC_{90}) causes complete killing of adherent cells at the longest times of cell growth, cisplatin at the concentration corresponding to IC_{90} fails to kill adherent cells completely even at the longest times of their growth (Fig. 2D).

DNA-bound iridium in cells

To confirm that **1** belongs to the class of DNA damaging agents, iridium levels on nuclear DNA were determined after the exposure of A2780 cells to 5 μM complex **1** for 24 h. The iridium content of nuclear DNA extracted from the A2780 cells

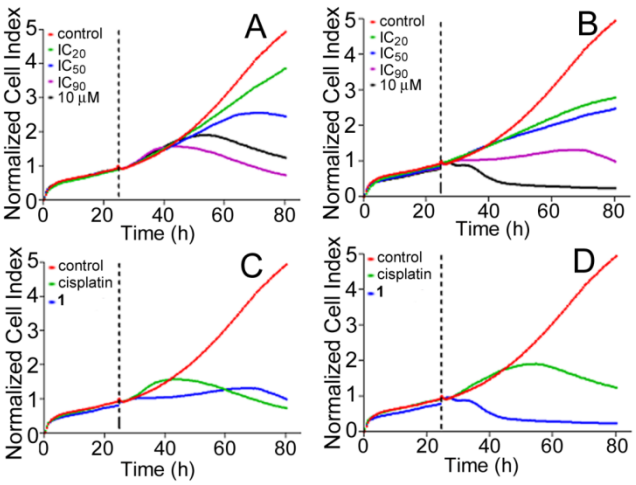

Fig. 2. Interactions of cisplatin (A) and **1** (B) with A2780 cells monitored by real-time cell analyzer (RTCA). For cisplatin: IC_{20} = 0.8 μM, IC_{50} = 2.8 μM, IC_{90} = 20 μM; for **1**: IC_{20} = 0.3 μM, IC_{50} = 0.8 μM, IC_{90} = 2.9 μM. The vertical lines indicate the start of treatment after allowing the cells to grow and adhere to the microelectrodes for 24 h. Cell indices were normalized to account for differences in cell counts that exist across the wells prior to treatment. Incubations were performed in triplicate with 10000 cells/well using inhibitory drug concentrations determined for 48 h of incubation in a colorimetric cell viability assay. (C, D) Time-dependent cell response profiles (TCRPs) for A2780 cells: untreated (control) and treated with **1** or cisplatin at their eqiutoxic IC_{90} (C) or equimolar (10 μM) (D) concentrations.

treated with **1** was found to be 79 ± 8 pg Ir/μg DNA (mean ± standard deviations for three independent samples), i.e. the metal content bound to DNA was approximately 13-fold greater than that from the cells treated with cisplatin (6 ± 1 pg Pt/μg DNA). Therefore, the new half-sandwich Ir(III) complex **1** is even more adept at targeting nuclear DNA than cisplatin. The amount of DNA-bound iridium in cells exposed to **1** parallels

the partition coefficients octanol/water obtained by the shake flask method (log P = 1.11 ± 0.17 or -2.21 ± 0.08 for **1**[6] or cisplatin,[22] respectively).

Cell-cycle analysis

The status of the cell cycle for cells treated with **1** and for comparative purposes also with cisplatin was analyzed. The analysis of cell cycle perturbation was performed using A2780 or HL-60 cells exposed to **1** or cisplatin at their equitoxic concentrations for 24, 48 or 72 h (Figs. S1A,B). An evaluation of the effects on cells produced by **1** or cisplatin in comparison with untreated control A2780 or HL-60 cells (Fig. 3) showed several significant differences in cell cycle modulation and these became more pronounced with increased concentration of the drug or increased period of incubation. Exposure of A2780 or HL-60 cells to cisplatin resulted in the appearance of a population in the sub-G_1 region of the profile, where apoptotic and necrotic cells are found. The occurrence of a sub-G_1 peak is consistent with the onset of internucleosomal DNA cleavage in late apoptosis.[23] Importantly, the sub-G_1 population for cells treated with **1** was significantly smaller than that for cells treated with cisplatin.

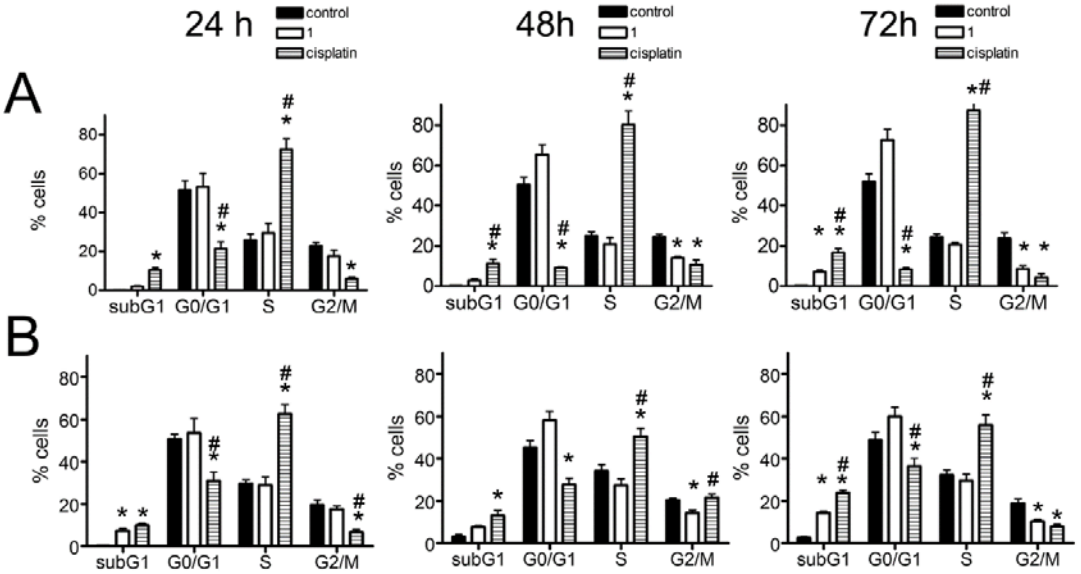

Fig. 3. Effects of **1** and cisplatin on cell cycle distribution of A2780(A) or HL-60 (B) cells. Untreated (control) cells or cells treated with equitoxic concentration (IC_{50}) of **1** or cisplatin for 24, 48, or 72 h were harvested, fixed, stained with propidium iodide, and assessed for cell cycle distribution by FACS analysis. The estimated percentages of A2780 (A) or HL-60 (B) cells in different phases of the cell cycle are indicated. The results are expressed as the mean ± SEM of three independent experiments. The symbol * denotes significant difference ($p < 0.05$) from the untreated control; # denotes the significant difference ($p < 0.05$) between **1** and cisplatin.

Also notably, treatment with **1** slightly, but significantly, increased the G_0/G_1 populations in contrast to cisplatin, which markedly decreased these populations. Similarly, treatment with **1** affected the peaks corresponding to the S phase negligibly in contrast to the peaks corresponding to this phase in case of treatment with cisplatin, which were increased significantly (Fig. 3). In addition, cisplatin caused a decrease of cell population in the G_2 phase in contrast to cells treated with **1** which displayed considerably smaller G_2 populations (Fig. 3). Thus, different effects were observed for the new half-sandwich Ir(III) complex **1** and cisplatin. The fact that **1** and cisplatin had different effects on cell cycle progression suggests different mechanisms of biological action for these two metal-based compounds, which is also consistent with the results of impedance-based real-time monitoring of the effects of these metallodrugs on cell growth (Fig. 2).

Annexin V-propidium iodide (PI) dual staining assay was also employed to quantify apoptosis induced by **1** in A2780 and HL-60 cancer cells after 24 or 48 h of incubation at equitoxic concentrations (IC_{90} values). Annexin V binds phosphatidyl serine residues, which are asymmetrically distributed toward the inner plasma membrane, but migrate to the outer plasma membrane during apoptosis.[24] Fig. 4 shows that treatment of HL-60 cells with **1** for 24 h induced a greater increase in the Annexin V-positive/PI-negative cell population (right bottom quadrant Q3) than treatment with cisplatin did (Fig. 4). The annexin V-positive/PI negative cell population constitutes the fraction of early apoptotic cells, and the percentage of cells undergoing early apoptosis can be calculated from the dots of the right bottom quadrants.[25] The data show that after 24 h of incubation, **1** induced early apoptosis in 22% of HL-60 cells, whereas cisplatin did not increase the population of cells in Q3 quadrant compared to control, untreated cells. For longer period of incubation (48 h), the percentage of cells undergoing an early apoptosis were 34 and 23% for **1** and cisplatin, respectively.

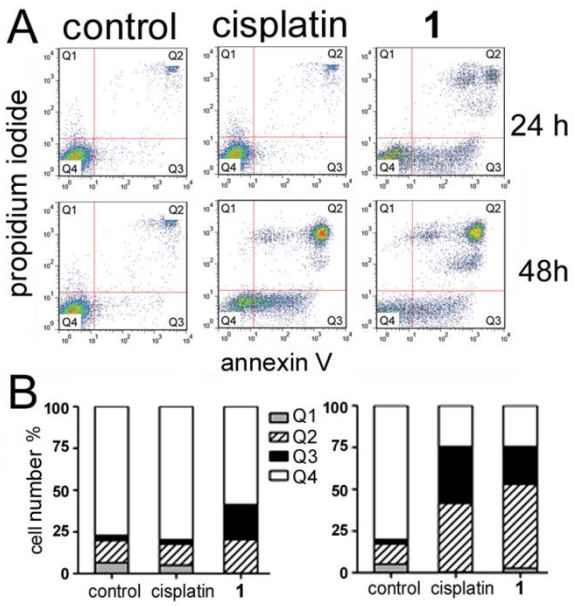

Fig. 4. Apoptosis of HL-60 cells after treatment with cisplatin or **1** as detected by Annexin V/PI. Cells were untreated (control) or treated with 3.2 μM ($IC_{90,48h}$) cisplatin or 1.8 μM ($IC_{90,48h}$) **1** for 24 or 48 h. A. Density plots. Early apoptotic cells are in the low right quadrant (Q3, annexin V-positive, PI-negative), whereas necrotic and late apoptotic cells are in the up-right quadrant (annexin V and PI-positive). The experiments were performed in triplicate. B. Bar charts of quantitative evaluation. Left chart: treatment for 24 h; right chart, treatment for 48 h. Quadrant 1, PI-positive (cells undergoing necrosis); Quadrant 2, Annexin V-positive /PI-positive (cells in the late period of apoptosis and undergoing necrosis); Quadrant 3, Annexin V positive/ PI-negative (cells in the early period of apoptosis); Quadrant 4, Annexin V – negative/ PI-negative (living cells).

Cell population distributed in right upper quadrant Q2 (PI positive/Anexin V positive cells) was also changed as a result of treatment of HL-60 cells with **1** or cisplatin. This population comprises the cells in the late period of apoptosis and undergoing secondary necrosis. Treatment with **1** increased the number of late apoptotic and necrotic cells after 24 and 48 h of treatment by 10% and 40%, respectively. In contrast, the Q2 fractions of HL-60 cells was not affected by 24 h of treatment with cisplatin, whereas 48 h of treatment with cisplatin induced an increase in the late apoptotic/necrotic fraction by 30% (Fig. 4C). Qualitatively similar results were obtained also for A2780 cells, in which the population of anexin V-positive/PI negative cells induced by **1** was higher than that induced by cisplatin even after 48 h of treatment (Fig. S2).

Cell death detection

To distinguish late apoptotic cells from those undergoing necrosis, DNA fragmentation induced by **1** and cisplatin (at various concentrations) over 24 h was quantified by a specific ELISA colorimetric kit. This analysis allows the appearance and relative amounts of cytoplasmic histone associated-DNA fragments (mono- and oligonucleosomes) to be measured after the induction of apoptosis or when these fragments are released from necrotic cells. Fig. 5 shows DNA fragmentation induced by equimolar (Figs. 5A,B) or equitoxic (Figs. 5C,D) concentrations of both **1** and cisplatin in A2780 and HL-60 cells as a result of apoptotic processes. These results demonstrate that treatment with both antitumor agents led to apoptotic events in both cell lines, the level of necrosis being significantly lower compared to apoptosis triggered by both metallodrugs. Importantly, **1** induced a significantly higher level of DNA fragmentation due to apoptosis in comparison with cisplatin in A2780 cells for both eqiutoxic and equimolar concentrations of metallodrugs used in these experiments (Fig. S3). In HL-60 cells, **1** was significantly more effective in inducing the apoptotic fragmentation than cisplatin at their equimolar concentrations, whereas both complexes at equitoxic concentrations exhibited a similar effect. A similar procedure was also used to detect the extent of necrosis induced by **1** or cisplatin (Fig. S3). Importantly, the level of necrosis was significantly lower compared to apoptosis triggered by both metallodrugs and in both A2780 and HL-60 cell lines (Fig. 5).

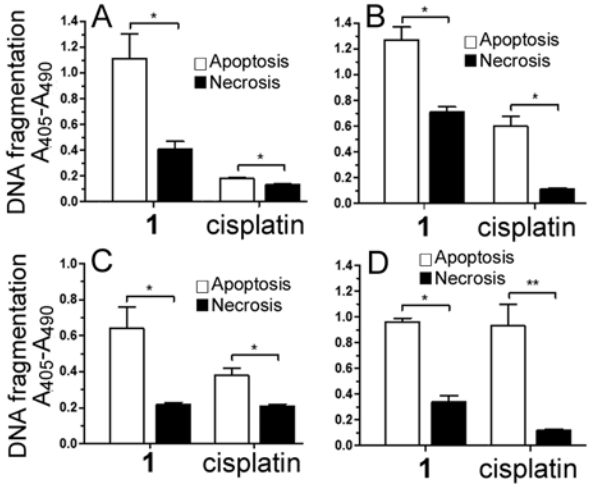

Fig. 5. Detection of apoptosis and necrosis in A2780 cells (A, C) or HL-60 cells (B, D). Cells were treated with equimolar (3 μM) (A, B) or equitoxic (IC_{50}) (C, D) concentrations of **1** or cisplatin for 24 h. The symbols * and ** denote significant difference ($p < 0.01$ and $p < 0.05$, respectively). Experiments were made in triplicate.

To further support the view that the cytotoxic action of **1** is associated with triggering of apoptosis, the genomic DNA from HL-60 cells exposed for 48 h at the equitoxic (IC_{50} and IC_{90}) or equimolar (10 μM) concentrations of **1** and cisplatin was extracted and analyzed by agarose gel electrophoresis. Treatment of HL-60 cells with **1** produced a ladder of genomic DNA as indicative of apoptosis (Fig. 6, lanes 6-8). A similar effect was observed also for cisplatin (Fig. 6, lanes 3-5).

Multi-parameter apoptosis assay

To identify biochemical events leading to characteristic changes occurring in apoptotic pathway induced by 1, multiparameter apoptosis assay was performed as well. This employs, TMRE as a probe for mitochondrial membrane potential, and Hoechst Dye to demonstrate nuclear morphology.

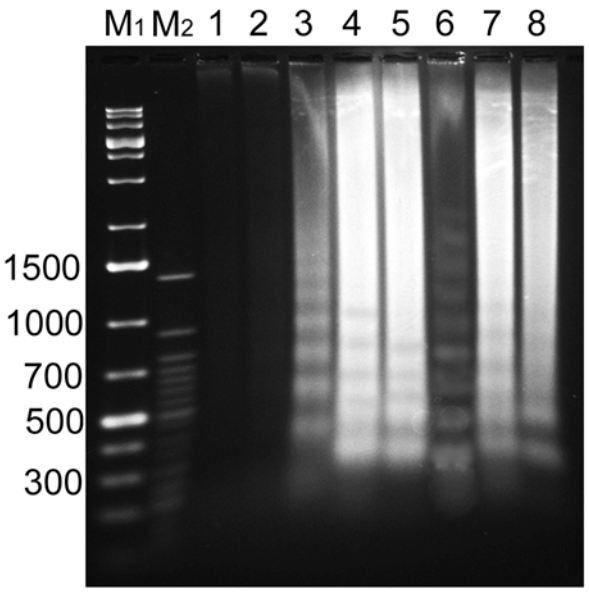

Fig. 6. Agarose gel electrophoresis of genomic DNA extracted from HL-60 cells treated with **1** or cisplatin. Lane 1, control, untreated cells; lane 2, cells treated with DMSO (0.1%); lanes 3-5, cells treated with cisplatin at its 0.97 μM ($IC_{50,48h}$), 3.2 μM ($IC_{90,48h}$) and 10 μM concentrations, respectively; lanes 6-8; cells treated with **1** at its 0.57 μM ($IC_{50,48h}$), 1.8 μM ($IC_{90,48h}$), and 10 μM concentrations, respectively. Lanes M1 and M2, DNA markers.

The assay allows phenotypic characterization of different cell death parameters at a single-cell level. Thus, the changes in nuclear morphology, mitochondrial potential and externalization of phospholipids as a hallmark of apoptosis were determined simultaneously after treatment of A2780 cells with **1** or cisplatin for 24 h. Complex **1** induced an increase of fluorescence intensity of nuclei (Figs. 7A and S4), and a decrease in mitochondrial membrane potential (Figs. 7B and S4) of A2780 cells as compared to the control, untreated cells. Changes in morphology, such as nuclear fragmentation, nuclear condensation, and presence of apoptotic bodies were also detectable (Fig. S4) as a result of treatment with **1**. Similar changes in nuclear morphology were observed also for the cells treated with cisplatin, indicating the presence of apoptotic cells. Interestingly, treatment with cisplatin resulted in a slight, but significant increase of fluorescence of TMRE (Figs. 7B and S4), suggesting the opposite effect on the mitochondrial membrane potential than that of **1**.

The perturbations in mitochondrial function associated with reduced mitochondrial membrane potential may result in the oxidative stress related to increased ROS generation. Therefore, 2´,7´-dichlorodihydrofluorescein diacetate (DCFH-DA) was used to measure the effect of **1** and, for comparative purposes, also of cisplatin on the production of ROS by A2780 human cancer cells. The DCFH-DA method is designed to provide a highly sensitive, quantifiable, real-time assessment of ROS production.19-20 To evaluate ROS formation, A2780 cells untreated or treated with 1 or cisplatin were incubated with 10 μM DCFH-DA for 30 min in the dark. DCFH-DA is cleaved by cellular esterases, oxidized by ROS and yields a fluorescent

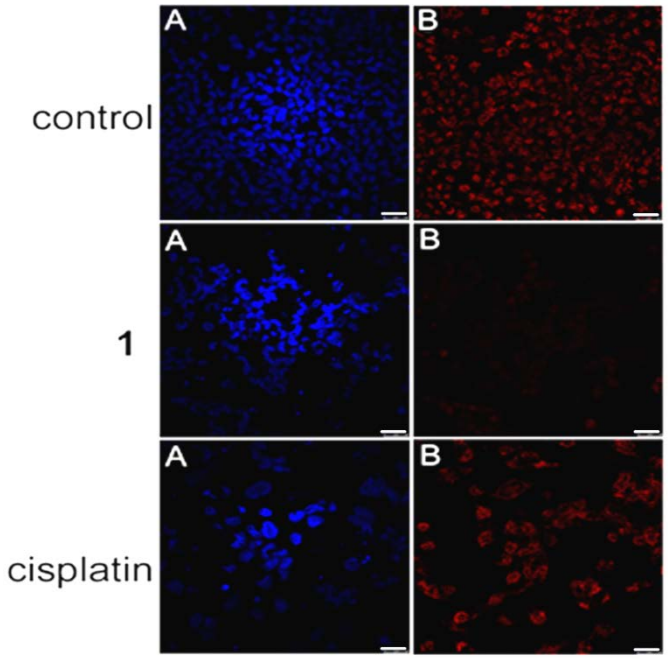

Fig. 7. Confocal microphotographs. A2780 cells untreated (top panels) or treated with **1** (middle panels) or cisplatin (bottom panels) were stained with (A) Hoechst dye for evaluation of nuclear morphology, (B) TMRE for changes in mitochondrial membrane potential. Scale bars represent 25 μm.

product. After incubation, the resulting fluorescence was measured and the data are plotted in Fig. 8.

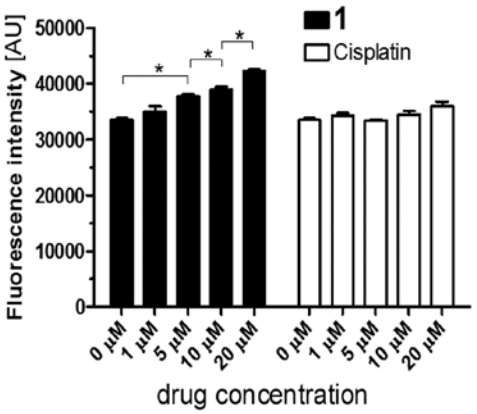

Fig. 8. Generation of ROS in A2780 cells induced by various concentrations of **1** or cisplatin. Statistically significant values ($p \leq 0.01$; highly significant) were evaluated using students t-test and signed with (*) at the top of the significant bars. Experiments were made in triplicate.

Treatment of A2780 cells with **1** resulted in concentration-dependent increase of fluorescence, indicating the production of ROS. In contrast, the effect of cisplatin on ROS production in treated cells was insignificant.

Discussion

The cytotoxicity profile of **1** is distinct from that of cisplatin in a panel of several well characterized cisplatin-sensitive and -resistant human cancer cell lines. In general, the activity of **1** was considerably higher than that of cisplatin in all tumor cells

tested in this work. Encouragingly, the activity of **1** was markedly higher than that of cisplatin in cisplatin-resistant cell lines (A2780/cisR, variant of A2780 cells with acquired resistance to cisplatin[26-27]) and the MCF-7 breast cancer cell line (with inherent cisplatin resistance[28]). The cisplatin-resistant A2780/cisR cells (with acquired cisplatin resistance) displayed a low level of resistance to **1** (IC_{50} for A2780, 0.22 μM; IC_{50} forA2780/cisR, 0.42 μM) compared to cisplatin (corresponding IC_{50} values of 0.81 and 3.8 μM). Similarly, the cisplatin-resistant MCF-7 cells (with inherent cisplatin resistance) displayed a low level of resistance to **1** (IC_{50} was 0.84 μM) compared to cisplatin (corresponding IC_{50} value was 9.3 μM). Notably, **1** differed greatly from cisplatin in that it was less toxic to healthy, nontumorigenic, normal human fibroblast cells and Chinese hamster ovary cells. For instance, the IC_{50} observed for **1** in nontumorigenic, normal human fibroblast cells was 25-fold higher than that in human ovarian carcinoma A2780 cells, whereas IC_{50} observed for cisplatin in nontumorigenic fibroblast cells was only 17-fold higher than that in ovarian carcinoma cells; Table 1). In other words, we observed a pronouncedly higher selectivity of **1** for tumor cells relative to the nontumorigenic, normal cells in comparison with conventional cisplatin.

Activation of cell cycle checkpoints is a general cellular response after exposure to cytotoxic agents. Previous studies have indicated that cisplatin and other platinum agents predominantly inhibit cell cycle progression at the S- and/or G_2/M phase.[29-30] Our studies, performed in the cell lines with wt p53 status (A2780) as well as in the cells with no intact p53 gene (HL-60), show differences between cisplatin and **1** at the level of cell cycle regulation (Fig.3). We found differences in type and dynamics of cell cycle perturbations induced by these two compounds. While cisplatin markedly blocks A2780 cells in the S-phase already after 24-h exposure, **1** induced a significant block in the G_0/G_1 phase, but only after 48-h exposure. It is therefore clear that **1** can arrest at the G_0/G_1-phase and disturb protein synthesis.[31]

The conclusion that there are differences in type and dynamics of cell cycle perturbations induced by **1** and cisplatin is also supported by the results of impedance-based real-time monitoring of the effects of these metal-based drugs on cell growth. In contrast to standard methods for determining cell viability or proliferation (e.g., SRB or MTT assays, etc.) representing end-point analysis of whole cell population, this method makes it possible to register very small and rapid changes in cell count, cell adhesion, and cell morphology due to drug toxicity. The results of these experiments indicate (Fig. 2) that both **1** and cisplatin produce a concentration-dependent decrease in impedance, suggesting that the reduced cell viability determined in the colorimetric assays translates into cell death. By contrast, an increase in cisplatin dose does not kill cells to an extent that would be expected from the IC_{90} values determined by SRB assay. More interestingly, **1** kills A2780 cells significantly more efficiently than cisplatin at equitoxic concentrations (IC_{90}) determined by the SRB assay. These findings suggest that critical differences exist in the rate and mechanisms of cell kill caused by the two agents. Previous studies have shown that platinum drugs, while generally believed to induce apoptotic cell death, may require concentrations significantly higher than IC_{50} values to produce the morphological features of apoptosis.[32] However, the preapoptotic signaling in various cancer cell lines has been demonstrated to be defective causing inefficient cell kill by cisplatin.[33]

It has been demonstrated[34] that impedance-based monitoring of cellular responses to biologically active small molecule compounds produces TCRPs, which can be predictive of mechanism of action of small molecules. The TCRP of cisplatin coclustered with the TCRPs of compounds interfering with DNA synthesis and replication, transcription, and translation, which are also known to induce cell-cycle arrest followed by the induction of cell death. Careful examination of the profile obtained for **1** (Fig. 2) revealed that its TCRP can be coclustered with the subcluster of DNA interfering compounds inhibiting protein translation and inducing cell cycle arrest at G_1 or S transition and subsequently cell death.[34] This nicely correlates with what has been deduced from cell cycle studies (*vide supra*), i.e. that **1** can arrest at the G_0/G_1-phase and disturb protein synthesis.[31]

The impedance-based monitoring of cellular responses to **1** suggested that the cytotoxicity of **1** could also result from mechanisms associated with nuclear DNA damage as in the case of cisplatin. This hypothesis is supported by the finding that the IC_{50} values of **1** and cisplatin (Table 1) correlate with the amount of iridium or platinum, respectively, found on the nuclear DNA of A2780 cells treated with **1** or cisplatin (Table 3). For instance, when the effects of **1** and cisplatin are compared at the same metal concentration (5 μM), **1** forms 13-fold more DNA adducts than cisplatin after 24 h of treatment of A2780 cells.

The implications of cell cycle disruption were explored by staining the cells with FITC-conjugated Annexin V for apoptosis detection and propidium iodide to detect necrosis (Figs. 4 and S2). The data indicate that **1** also displays an apoptotic mechanism of action, as occurs for cisplatin. In addition, **1** showed a superior ability to induce early apoptosis already after 24 h in comparison with cisplatin. Hence, these data suggest that **1** acts more quickly than cisplatin to induce cell death and that **1** is more effective apoptosis inducer than cisplatin in particular in early stages of treatment, when the apoptotic effects predominate over the necrosis. In later stages, the population of late apoptotic/necrotic cells is also significantly increased. These conclusions were further supported by the results quantifying DNA fragmentation induced by **1** and cisplatin by a specific ELISA colorimetric kit (Figs. 5 and S3) and agarose gel electrophoresis (Fig. 6). The results shown in Fig. 5 also demonstrated that treatment with both metal-based agents led to apoptotic events in the cell lines tested in the present work, the level of necrosis being significantly lower compared to apoptosis triggered by both metallodrugs.

TMRE is used to label active mitochondria. TMRE is a cell permeant that readily accumulates in active mitochondria due to their relative negative charge. Depolarized or inactive mitochondria have decreased membrane potentials and fail to sequester TMRE. The treatment of A2780 cells with **1** resulted in a marked reduction of fluorescence of TMRE (Figs. 7B and S4) indicative of mitochondrial membrane disruption. This phenomenon was not observed in cisplatin-treated cells. This observation suggests that **1** can indeed cause disruption of mitochondrial function and associate production of reactive oxygen species (ROS) consistent with previous suggestion[13] highlighting the involvement of organometallic half-sandwich iridium complexes in ROS production (Fig. 8). Hence, **1** can induce apoptosis in a dual manner causing both nuclear DNA damage and mitochondrial dysfunction. A plausible support for the thesis that **1** plays a role in making cisplatin-resistant cells susceptible toward treatment with this half-sandwich iridium complex and its derivatives[13] may be associated with this dual mechanism of apoptosis induction. The cells are likely to develop resistance much less easily to two mechanisms simultaneously than to only one mechanism so that for instance repeated administration would not have to lead to acquired resistance so easily as in the case of cisplatin treatment. Thus, application of **1** and its iridium derivatives remain an attractive therapeutic strategy for attacking cisplatin-resistant tumors.

In conclusion, the experimental data described in the present work demonstrate that the new half-sandwich Ir(III) complex **1** displays dual effects in killing cancer cells causing nuclear DNA damage and mitochondrial dysfunction involving ROS production simultaneously. This conclusion is consistent with previous COMPARE-based predictive findings.[13] In addition, **1** displays superior efficacy in cell killing than cisplatin. It also appears to retain significant activity in human tumor cell lines and xenografts that are refractory or poorly responsive to cisplatin, and displays a high activity in human tumor cell lines that are characterized by both wild type and mutant p53 gene. In contrast, on average, cells with mutant p53 are more resistant to the effect of cisplatin. Moreover, the data obtained in the present work suggest that **1** is a promising candidate for further development in the treatment of cisplatin-resistant cells. Thus, **1** and its iridium derivatives remain promising compounds for the generation of novel anticancer non-platinum drug candidates with higher efficacy, improved therapeutic index and different cytotoxicity profiles than those of platinum drugs currently used in the clinic.

Acknowledgements

This research was supported by the Academy of Sciences of the Czech Republic (Grant M200041201) and the ERC (Grant No. 247450 to P.J.S.). Research of V.N. was also supported by the student project of the Palacky University in Olomouc (Grant PrF 2014 029). J.K.'s research was also supported by Operational Program Education for Competitiveness - European Social Fund (CZ 1.07/2.3.00/20.0057) of the Ministry of Education, Youth and Sports of the Czech Republic. The authors acknowledge that their participation in the EU COST Action CM1105 enabled them to exchange regularly the most recent ideas in the field of metallodrugs with several European colleagues. The authors also declare that P.J.S. is a named inventor on a patent application on organometallic iridium anticancer complexes filed by the University of Warwick. The authors also thank Dr. Jitka Pracharova from Department of Biophysics, Palacky University in Olomouc for performing cytotoxicity experiments with human skin fibroblasts (primary cell culture).

Notes and references

[a] *Institute of Biophysics, Academy of Sciences of the Czech Republic, v.v.i., Kralovopolska 135, CZ-61265 Brno, Czech Republic. Fax: +420 541240499; Tel: +420 541517148; E-mail: brabec@ibp.cz*
[b] *Department of Biophysics, Faculty of Science, Palacky University, 17. listopadu 12, CZ-77146 Olomouc, Czech Republic*
[c] *Department of Chemistry, University of Warwick, Gibbet Hill Road, Coventry CV4 7AL, United Kingdom*
[d] *Current address: Department of Chemistry, University of Basel, Spitalstrasse 51, 4056 Basel, Switzerland*

1 P. C. Bruijnincx and P. J. Sadler, New trends for metal complexes with anticancer activity. *Curr. Opin. Chem. Biol.* 2008, 12. 197-206.
2 K. S. Lovejoy and S. J. Lippard, Non-traditional platinum compounds for improved accumulation, oral bioavailability, and tumor targeting. *Dalton Trans.* 2009. 10651 - 10659.
3 G. Gasser, I. Ottand and N. Metzler-Nolte, Organometallic anticancer compounds. *J. Med. Chem.* 2011, 54. 3-25.
4 N. P. E. Barry and P. J. Sadler, Exploration of the medical periodic table: towards new targets. *Chem. Commun.* 2013, 49. 5106-5131.
5 Z. Liu, A. Habtemariam, A. M. Pizarro, G. J. Clarkson and P. J. Sadler, Organometallic iridium(III) cyclopentadienyl anticancer complexes containing C,N-chelating ligands. *Organometallics* 2011, 30. 4702-4710.
6 Z. Liu, L. Salassa, A. Habtemariam, A. M. Pizarro, G. J. Clarkson and P. J. Sadler, Contrasting reactivity and cancer cell cytotoxicity of isoelectronic organometallic iridium(III) complexes. *Inorg. Chem.* 2011, 50. 5777-5783.
7 Z. Liu, A. Habtemariam, A. M. Pizarro, S. A. Fletcher, A. Kisova, O. Vrana, L. Salassa, P. C. A. Bruijnincx, G. J. Clarkson, V. Brabec and P. J. Sadler, Organometallic half-sandwich iridium anticancer complexes. *J. Med. Chem.* 2011, 54. 3011-3026.
8 A. Kastl, A. Wilbuer, A. L. Merkel, L. Feng, P. Di Fazio, M. Ockerand E. Meggers, Dual anticancer activity in a single compound: visible-light-induced apoptosis by an antiangiogenic iridium complex. *Chem. Commun.* 2012, 48. 1863-1865.
9 J. Ruiz, V. Rodriguez, N. Cutillas, K. G. Samper, M. Capdevila, O. Palacios and A. Espinosa, Novel C,N-chelate rhodium(III) and iridium(III) antitumor complexes incorporating a lipophilic steroidal conjugate and their interaction with DNA. *Dalton Trans.* 2012, 41. 12847-12856.
10 V. Novohradsky, Z. Liu, M. Vojtiskova, P. J. Sadler, V. Brabec and J. Kasparkova, Mechanism of cellular accumulation of an iridium(III) pentamethylcyclopentadienyl anticancer complex containing a C,N-chelating ligand. *Metallomics* 2014, 6. 682-690.
11 Z. Liu, I. Romero-Canelón, B. Qamar, J. M. Hearn, A. Habtemariam, N. P. E. Barry, A. M. Pizarro, G. J. Clarkson and

P. J. Sadler, The potent oxidant anticancer activity of organoiridium catalysts. *Angew. Chem. Int. Ed.* 2014, 53. 3941-3946.
12 Z. Almodares, S. J. Lucas, B. D. Crossley, A. M. Basri, C. M. Pask, A. J. Hebden, R. M. Phillips and P. C. McGowan, Rhodium, iridium, and ruthenium half-sandwich picolinamide complexes as anticancer agents. *Inorg. Chem.* 2014, 53. 727-736.
13 J. M. Hearn, I. Romero-Canelon, B. Qamar, Z. Liu, I. Hands-Portman and P. J. Sadler, Organometallic iridium(III) anticancer complexes with new mechanisms of action: NCI-60 screening, mitochondrial targeting, and apoptosis. *ACS Chem. Biol.* 2013, 8. 1335-1343.
14 N. P. Johnson, J.-L. Butour, G. Villani, F. L. Wimmer, M. Defais, V. Pierson and V. Brabec, Metal antitumor compounds: The mechanism of action of platinum complexes. *Prog. Clin. Biochem. Med.* 1989, 10. 1-24.
15 E. R. Jamieson and S. J. Lippard, Structure, recognition, and processing of cisplatin-DNA adducts. *Chem. Rev.* 1999, 99. 2467-2498.
16 V. Brabec, DNA modifications by antitumor platinum and ruthenium compounds: their recognition and repair. *Prog. Nucleic Acid Res. Mol. Biol.* 2002, 71. 1-68.
17 Z. Liu, A. Habtemariam, A. M. Pizarro, S. A. Fletcher, A. Kisova, O. Vrana, L. Salassa, P. C. A. Bruijnincx, G. J. Clarkson, V. Brabec and P. J. Sadler, Organometallic half-sandwich iridium anticancer complexes. *J. Med. Chem.* 2011, 54. 3011-3026.
18 J. P. Gong, F. Traganos and Z. Darzynkiewicz, A selective procedure for DNA extraction from apoptotic cells applicable for gel electrophoresis and flow cytometry. *Anal. Biochem.* 1994, 218. 314-319.
19 J. P. Robinson, L. H. Bruner, C. F. Bassoe, J. L. Hudson, P. A. Ward and S. H. Phan, Measurement of intracellular fluorescence of human-monocytes relative to oxidative-metabolism. *J. Leukocyte Biol.* 1988, 43. 304-310.
20 B. Kalyanaraman, V. Darley-Usmar, K. J. A. Davies, P. A. Dennery, H. J. Forman, M. B. Grisham, G. E. Mann, K. Moore, L. J. Roberts and H. Ischiropoulos, Measuring reactive oxygen and nitrogen species with fluorescent probes: challenges and limitations. *Free Radic. Biol. Med.* 2012, 52. 1-6.
21 V. Vichain and K. Kirtikara, Sulforhodamine B colorimetric assay for cytotoxicity screening. *Nat. Protocols* 2006, 1. 1112-1116.
22 A. F. Westendorf, L. Zerzankova, L. Salassa, P. J. Sadler, V. Brabec and P. J. Bednarski, Influence of pyridine versus piperidine ligands on the chemical, DNA binding and cytotoxic properties of light activated trans, trans, trans-$[Pt(N_3)_2(OH)_2(NH_3)(L)]$. *J. Inorg. Biochem.* 2011, 105. 652–662.
23 K. Clodi, K. O. Kliche, S. R. Zhao, D. Weidner, T. Schenk, U. Consoli, S. W. Jiang, V. Snell and M. Andreeff, Cell-surface exposure of phosphatidylserine correlates with the stage of fludarabine-induced apoptosis in chronic lymphocytic leukemia and expression of apoptosis-regulating genes. *Cytometry* 2000, 40. 19-25.
24 M. A. Fuertes, J. Castilla, C. Alonso and J. M. Perez, Cisplatin biochemical mechanism of action: From cytotoxicity to induction of cell death through interconnections between apoptotic and necrotic pathways. *Curr. Med. Chem.* 2003, 10. 257-266.
25 M. van Engeland, L. J. W. Nieland, F. C. S. Ramaekers, B. Schutte and C. P. M. Reutelingsperger, Annexin V-affinity assay: A review on an apoptosis detection system based on phosphatidylserine exposure. *Cytometry* 1998, 31. 1-9.
26 L. R. Kelland, C. F. J. Barnard, K. J. Mellish, M. Jones, P. M. Goddard, M. Valenti, A. Bryant, B. A. Murrer and K. R. Harrap, A novel trans-platinum coordination complex possessing in vitro and in vivo antitumor activity. *Cancer Res.* 1994, 54. 5618-5622.
27 L. R. Kelland, S. Y. Sharp, C. F. ONeill, F. I. Raynaud, P. J. Beale and I. R. Judson, Mini-review: discovery and development of platinum complexes designed to circumvent cisplatin resistance. *J. Inorg. Biochem.* 1999, 77. 111-115.
28 S. J. Fan, M. L. Smith, D. J. Rivet, D. Duba, Q. M. Zhan, K. W. Kohn, A. J. Fornace and P. M. O'Connor, Disruption of p53 function sensitizes breast cancer MCF-7 cells to cisplatin and pentoxifylline. *Cancer Res.* 1995, 55. 1649-1654.
29 M. Ormerod, C. O'Neill, D. Robertson, L. Kelland and K. Harrap, cis-Diamminedichloroplatinum(II)-induced cell death through apoptosis in sensitive and resistant human ovarian carcinoma cell lines. *Cancer Chemother. Pharmacol.* 1996, 37. 463-471.
30 Z. H. Siddik, Cisplatin: mode of cytotoxic action and molecular basis of resistance. *Oncogene* 2003, 22. 7265-7279.
31 C. Van den Bogert, G. Van Kernebeek, L. De Leij and A. M. Kroon, Inhibition of mitochondrial protein synthesis leads to proliferation arrest in the G1-phase of the cell cycle. *Cancer Lett.* 1986, 32. 41-51.
32 C. F. O'Neill, M. G. Ormerod, D. Robertson, J. C. Titley, Y. Cumber-Walsweer and L. R. Kelland, Apoptotic and non-apoptotic cell death induced by cis and trans analogues of a novel ammine(cyclohexylamine)dihydroxodichloroplatinum(IV) complex. *British J. Cancer* 1996, 74. 1037-1045.
33 V. M. Gonzalez, M. A. Fuertes, C. Alonso and J. M. Perez, Is cisplatin-induced cell death always produced by apoptosis? *Mol. Pharmacol.* 2001, 59. 657-663.
34 Y. A. Abassi, B. Xi, W. F. Zhang, P. F. Ye, S. L. Kirstein, M. R. Gaylord, S. C. Feinstein, X. B. Wang and X. Xu, Kinetic cell-based morphological screening: Prediction of mechanism of compound action and off-target effects. *Chem. Biol.* 2009, 16. 712-723.

Footnotes

† Electronic supplementary information (ESI) available. See DOI:

‡ These authors equally contributed to the paper.